Syntheses, Molecular Structures, and Spectroscopy of Gold(III) Dithiolate Complexes

M. Adnan Mansour,[†] Rene J. Lachicotte,[†] Henry J. Gysling,[‡] and Richard Eisenberg*,[†]

NSF−Science and Technology Center for Photoinduced Charge Transfer, Department of Chemistry, University of Rochester, Rochester, New York 14627-0216, and Imaging Research and Advanced Development, Eastman Kodak Company, Rochester, New York 14650-2109

Received January 13, 1998

Two Au(III) dithiolate complexes, [Au(dbbpy)(tdt)]PF_6 and Au(η^2-*C,N*-ppy)(tdt), (dbbpy = 4,4′-di-*tert*-butyl-2,2′-bipyridine; tdt = 3,4-toluenedithiolate; ppy = C-deprotonated 2-phenylpyridine), have been prepared and structurally characterized by X-ray crystallography. The complexes have low-energy absorption bands that exhibit mild solvatochromism (λ_{max} = 444 nm (ϵ, 2310 M^{-1} cm^{-1}) in CH_2Cl_2 and 406 nm (ϵ, 3170 M^{-1} cm^{-1}) in DMSO) and are tentatively assigned to a charge-transfer-to-diimine transition. This transition occurs at higher energy than the analogous charge-transfer transition in related Pt(II) complexes (e.g., Pt(dbbpy)(tdt), λ_{max} = 563 nm (ϵ, 7200 M^{-1} cm^{-1}). Whereas neither Au(III) complex is emissive, their respective dichloride precursors, [Au(dbbpy)Cl_2]PF_6 and Au(η^2-*C,N*-ppy)Cl_2, luminesce in low-temperature glass matrixes from an excited state that is tentatively assigned as intraligand $\pi-\pi^*$. The neutral complex, Au(η^2-*C,N*-ppy)(tdt), is more easily oxidized (E_{ox} = 0.925 V vs 1.589 V (vs NHE)) and less easily reduced (E_{red} = −1.339 V vs −0.255 V (vs NHE)) than the cationic complex, [Au(dbbpy)(tdt)]PF_6. Both dithiolate complexes exhibit approximately square planar coordination. Yellow crystals of [Au(dbbpy)(tdt)]PF_6 ($C_{25}H_{30}AuF_6N_2PS_2$) are triclinic, space group $P\bar{1}$ (No. 2), with a = 7.1977(2) Å, b = 11.7292(1) Å, c = 17.5820(5) Å, α = 104.537(2)°, β = 96.592(2)°, γ = 102.455(2)°, V = 1380.41(6) $Å^3$, Z = 2, and final R = 0.050 (R_w = 0.1062) for 3446 unique reflections. Orange crystals of Au(η^2-*C,N*-ppy)(tdt) ($C_{18}H_{14}AuNS_2$) are monoclinic, space group $P2_1/c$ (No. 14), with a = 8.852(1) Å, b = 11.726(2) Å, c = 15.499(5) Å, β = 101.34(2)°, V = 1577.5(6) $Å^3$, Z = 4, and final R = 0.0438 (R_w = 0.0759) for 3685 unique reflections. A structural trans effect in Au(η^2-*C,N*-ppy)(tdt) results in a significantly longer Au−S distance (ca. 0.1 Å) trans to the Au−C bond than that trans to the Au−N bond. In the solid state, the $[Au(dbbpy)(tdt)]^+$ cations are arranged in stacks with alternating intermolecular Au···Au separations of 3.60 and 3.75 Å while the Au(η^2-*C,N*-ppy)(tdt) molecules form stacks with an intermolecular Au···Au separation of 3.81 Å.

Introduction

In contrast to extensive studies on the photochemical and photophysical properties of Au(I) complexes,[1] few investigations of this type have been conducted on related Au(III) complexes. Interest in luminescent members of this group of complexes lies in their potential use as photosensitizers or photocatalysts for the activation of small molecules and the promotion of organic reactions,[2] in the conversion of sunlight into stored chemical energy,[3] as nonlinear optical materials,[4] and as photoluminescent probes in biological systems.[5] In this report, we describe a study of Au(III) complexes that are isoelectronic with diimine dithiolate complexes of Pt(II), a novel and interesting class of solvatochromic and solution-luminescent d^8 metal complexes. Through extensive study of these Pt(II) diimine dithiolate complexes,[6] it has been determined that the highest occupied molecular orbital (HOMO) is largely Pt(d)/S(p)/dithiolate in character while the lowest unoccupied molecular orbital (LUMO) is a π^* orbital of the diimine, leading to a low-energy charge-transfer-to-diimine excited state. This charge-transfer (CT) transition, coupled with a highly polar

[†] University of Rochester.
[‡] Eastman Kodak Company.

(1) See for example: (a) McClesky, T. M.; Gray, H. B. *Inorg. Chem.* **1992**, *31*, 1733. (b) Forward, J. M.; Assefa, Z.; Fackler, J. P. *J. Am. Chem. Soc.* **1995**, *117*, 9103. (c) Tzeng, B. C.; Che, C.-M.; Peng, S. M. *J. Chem. Soc., Dalton Trans.* **1996**, 1769. (d) Yam, V. W. W.; Choi, S. W. K. *J. Chem. Soc., Dalton Trans.* **1996**, 4227. (e) Larson, L. J.; McCauley, E. M.; Weissbart, B.; Tinti, D. S. *J. Phys. Chem.* **1995**, *99*, 7218. (f) Hanna, S. D.; Zink, J. I. *Inorg. Chem.* **1996**, *35*, 297.

(2) (a) Ford, P. C.; Boese, W.; Lee, B.; MacFarlane, K. In *Photosensitization and Photocatalysis Using Inorganic and Organometallic Compounds*; Kalyanasundaram, K., Graetzel, M., Eds.; Kluwer Academic Publishers: Dodrecht, The Netherlands, 1993; pp 359−390. (b) Ford, P. C.; Friedman, A. In *Photocatalysis: Fundamentals and Applications*; Serpone, N., Pelizzetti, E., Eds.; J. Wiley and Sons: New York, 1989; Chapter 16. (c) Pelizetti, E.; Serpone, N. *Homogeneous and Heterogeneous Photocatalysis*; Pelizetti, E., Serpone, N., Eds.; D. Reidel Publishing: Dordrecht, Holland, 1985.

(3) Meyer, T. J. *Acc. Chem. Res.* **1989**, *22*, 163.

(4) Prasad, P. N.; Reinhardt, B. A. *Chem. Mater.* **1990**, *2*, 660.

(5) (a) Barton, J. K. *Commun. Inorg. Chem.* **1985**, 32. (b) Kumar, C. V.; Barton, J. K.; Turro, N. J. *J. Am. Chem. Soc.* **1985**, *107*, 5518. (c) Barton, J. K.; Goldberg, J. M.; Kumar, C. V.; Turro, N. J. *J. Am. Chem. Soc.* **1986**, *108*, 2081. (d) Friedman, A. E.; Chambron, J.-C.; Sauvage, J.-P.; Turro, N. J.; Barton, J. K. *J. Am. Chem. Soc.* **1990**, *112*, 4960. (e) Murphy, C. J.; Arkin, M. R.; Ghatlia, N. D.; Bossman, S. H.; Turro, N. J.; Barton, J. K. *Science* **1993**, *262*, 1025. (f) Murphy, C. J.; Arkin, M. R.; Ghatlia, N. D.; Bossman, S. H.; Turro, N. J.; Barton, J. K. *Proc. Natl. Acad. Sci. U.S.A.* **1994**, *91*, 5315. (g) Stemp, E. D. A.; Arkin, M. R.; Barton, J. K. *J. Am. Chem. Soc.* **1995**, *117*, 2375.

(6) (a) Cummings, S. D.; Eisenberg, R. *J. Am. Chem. Soc.* **1996**, *118*, 1949. (b) Cummings, S. D.; Eisenberg, R. *Inorg. Chem.* **1995**, *34*, 2007. (c) Zuleta, J.; Burberry, M. S.; Eisenberg, R. *Coord. Chem. Rev.* **1990**, *97*, 47.

(7) Yam, V. W. W.; Choi, S. W.-K.; Lai, T.-F.; Lee, W.-K. *J. Chem. Soc., Dalton Trans.* **1993**, 1001.

(8) Chan, C.-W.; Wong, W.-T.; Che, C.-M. *Inorg. Chem.* **1994**, *33*, 1266.

S0020-1669(98)00032-9 CCC: $15.00
Published on Web 08/20/1998

ground state, results in negative solvatochromic behavior. Through changes in ligand substituents that affect ligand electron-donating and -accepting properties, we have shown that the excited-state energies, redox potentials, electron transfer quenching rate constants, and relaxation dynamics can be systematically controlled.[6a]

As a logical step in the process of correlating excited-state properties with molecular design features, we have turned our focus to isoelectronic Au(III) diimine dithiolate systems. In previous reports of luminescent Au(III) complexes, Yam et al.[7] have investigated the photophysics of $[Au(diimine)L_2]^+$ systems, where diimine = 2,2′-bipyridine or 1,10-phenanthroline and L = mesityl or $-CH_2SiMe_3$, while Che and co-workers[8] have examined the cyclometalated derivatives $[Au(N^\frown N^\frown C)Cl]^+$, where $N^\frown N^\frown C$ = C-deprotonated 2,9-diphenylphenanthroline and 2,2′,2″-terpyridine analogues. Even with good σ-donor ligands such as mesityl or (trimethylsilyl)methyl, the luminescence observed by Yam for the diimine complexes was attributed to an intraligand $\pi-\pi^*$ charge-transfer transition.

The present study reports the synthesis, molecular structure determination, and spectroscopic characterization of the Au(III) complexes [Au(dbbpy)(tdt)]PF_6 and Au(η^2-*C*,*N*-ppy)(tdt) (tdt = 3,4-toluenedithiolate; dbbpy = 4,4′-di-*tert*-butyl-2,2′-bipyridine; ppy = C-deprotonated 2-phenylpyridine). The neutral cyclometalated complex Au(η^2-*C*,*N*-ppy)(tdt) makes possible a direct comparison of its potential solvatochromic behavior with that of the Pt(II) diimine dithiolate systems. Additionally, it was anticipated that the C-deprotonated ppy ligand would modify the electronic structure of the d^8 square-planar diimine complexes by virtue of its asymmetry and strong σ-donating phenyl carbon atom. The use of orthometalating ligands to alter the excited-state properties of metal complexes has been reported for other Pt(II), Pd(II), Ir(III), and Rh(III) complexes.[9] Orthometalation tends to destabilize ligand-field d−d excited states,[10] possibly leading to lowest energy CT excited states.

Experimental Section

Chemicals. 2-Phenylpyridine (Hppy) (Aldrich), 3,4-toluenedithiol (H_2tdt) (Aldrich), and K[$AuCl_4$] (Strem) were used as received. 4,4′-Di-*tert*-butyl-2,2′-bipyridine[11] (dbbpy) and Au(η^2-*C*,*N*-ppy)Cl_2[12] (ppy = C-deprotonated 2-phenylpyridine) were prepared according to literature procedures. Reagent grade acetone, acetonitrile, diethyl ether (Et_2O), and 2-propanol (ipa) were deoxygenated with an N_2 purge but otherwise used as received from Aldrich or Fisher Chemical. Spectroscopic grade *N*,*N*-dimethylformamide (DMF), methanol (MeOH), and dichloromethane (CH_2Cl_2) were used as received from Burdick and Jackson.

Preparation of Au(η^2-*C*,*N*-ppy)(tdt). In a 50 mL Schlenk flask, a solution of KOH (0.056 g, 1.0 mmol) in degassed MeOH (5 mL) was prepared. To this solution was added toluenedithiol (0.078 g, 0.50 mmol), and the mixture was allowed to stir at room temperature for 30 min. In a separate 50 mL Schlenk flask, a solution of Au(η^2-*C*,*N*-ppy)Cl_2 (0.160 g, 0.38 mmol) in warm, degassed DMF (10 mL) was prepared. The toluenedithiolate solution was then added to the Au(η^2-*C*,*N*-ppy)Cl_2 solution via cannula transfer. The color of the reaction mixture became bright orange immediately. After the solution was stirred at room temperature for 15 min, a precipitate began to form. The reaction was allowed to proceed at room temperature overnight. A bright orange solid was filtered from the reaction mixture, washed with hexanes (25 mL), Et_2O (25 mL), and then 1:1 ipa/H_2O (25 mL), and dried in vacuo. The orange powder was recrystallized from DMF/Et_2O at −18 °C. Yield = 0.131 g (68%). ^{1}H NMR (DMSO-d_6; δ): 8.88 (d, 1 H); 8.45 (d, 1 H); 8.34 (t, 1 H); 8.10 (d, 1 H); 7.71 (m, 2 H); 7.44 (m, 2 H); 7.11 (br m, 2 H); 6.74 (t, 1 H); 2.24 and 2.23 (2 s, 3 H). Anal. Calcd for $C_{18}H_{14}AuNS_2$: C, 42.78; H, 2.79; N, 2.77. Found: C, 42.60; H, 2.95; N, 2.76. MS (*m*/*z*): M^+ (507).

Preparation of [Au(dbbpy)Cl_2]PF_6. To a solution of K[$AuCl_4$] (0.268 g, 0.71 mmol) and KPF_6 (2.6 g, 14.1 mmol) in H_2O (25 mL) was added a solution of dbbpy (0.190 g, 0.71 mmol) in acetone (5 mL) dropwise. A bright yellow precipitate formed immediately upon addition. The reaction mixture was allowed to stir at room temperature for 3 h at which point the color had discharged to give a very pale yellow solid. The precipitate was filtered off, washed with H_2O (200 mL), hexanes (50 mL), and Et_2O (75 mL), and then dried in vacuo. Yield = 0.427 g (88%). ^{1}H NMR (DMSO-d_6; δ): 9.24 (d, 2 H); 8.91 (s, 2 H); 8.08 (d, 2 H); 1.46 (s, 18 H). IR (KBr): ν_{PF} = 835 (vs), 558 (m) cm^{-1}. Anal. Calcd for $C_{18}H_{24}AuCl_2F_6N_2P$: C, 31.73; H, 3.52; N, 4.11. Found: C, 31.62; H, 3.35; N, 4.04. MS (*m*/*z*): M^+ (536).

Preparation of [Au(dbbpy)(tdt)]PF_6. In a 50 mL Schlenk flask, a solution of [Au(dbbpy)Cl_2]PF_6 (0.102 g, 0.150 mmol) in degassed CH_3CN (5 mL) was prepared. In a separate 50 mL Schlenk flask, a solution of KOH (0.018 g, 0.32 mmol) in degassed MeOH (5 mL) was prepared and 3,4-toluenedithiol (0.029 g, 0.19 mmol) was added to it. After 30 min, the toluenedithiolate solution was added to the [Au(dbbpy)Cl_2]PF_6 solution. The color immediately changed from faint yellow to brown upon addition, becoming opaque. After 5 min, a dark brown precipitate began to form. The reaction mixture was allowed to stir at room temperature for 2.5 h. The solvent was removed in vacuo, and the residual solid was redissolved in CH_3CN and filtered through a plug of Celite which was then washed with CH_3CN until the washings were colorless. The deep yellow filtrate was concentrated, and Et_2O was added to give 0.057 g (42%) of fine, yellow needles. ^{1}H NMR (DMSO-d_6; δ): 8.95 (s, 2 H); 8.93 (d, 2 H); 8.06 (br m, 2 H); 7.07 (d, 1 H); 6.99 (s, 1 H); 6.89 (d, 1 H); 2.27 (s, 3 H); 1.47 (s, 18 H). IR (KBr): ν_{PF} = 841 (vs), 558 (m) cm^{-1}. Anal. Calcd for $C_{25}H_{30}AuF_6N_2PS_2$ ([Au(dbbpy)(tdt)]PF_6): C, 39.27; H, 3.95; N, 3.66. Found: C, 39.08; H, 3.84; N, 3.63. MS (*m*/*z*): M^+ (619); $M^+ + PF_6$ (764).

Physical Measurements. ^{1}H NMR spectra were recorded on a Bruker AMX-400 spectrometer operating at 400 MHz. Chemical shifts are reported relative to TMS but were measured based on residual proton solvent resonances (DMSO-d_6, δ 2.49; $(CD_3)_2CO$, δ 2.04). Infrared spectra were recorded on a Mattson Galaxy 6020 FTIR spectrophotometer as KBr pellets. Thermal gravimetric analyses (TGA) were recorded on a TA Instruments model 2950 TGA run by a TA Instruments computer system. The heating rate was 10 °C/min with a N_2 purge gas rate of 60 cm^3/min. Absorption spectra were recorded on a Hitachi U2000 UV−visible spectrophotometer. Steady-state emission measurements were performed on a Spex Fluorolog-2 fluorescence spectrophotometer equipped with a 450 W xenon lamp and Hamamatsu R929 photomultiplier tube detector. Room-temperature measurements were made using 1 cm × 1 cm quartz fluorescence cells; solutions were freeze−pump−thaw degassed 5 times. Low-temperature emission spectra were recorded in DMM (1:1:1 DMF−CH_2Cl_2−MeOH) solvent glasses formed in 4 mm diameter quartz EPR tubes placed in a liquid nitrogen dewar equipped with quartz windows. Emission was collected at 90° from the excitation for both experiments. Field desorption mass spectra (FDMS) were measured on a JEOL JMS-HX110 double focusing mass spectrometer (Kodak Research Laboratories); the molecular ion peaks reported correspond to the most intense peak in a polyisotopic pattern. Elemental analyses were performed by the Analytical Technology Division, Kodak Research Laboratories.

Electrochemical Measurements. Cyclic voltammograms were measured using an EG&G PAR model 263A potentiostat which was controlled by model 270/250 Research Electrochemistry Software, V. 4.10, supplied by EG&G Instruments. The cyclic voltammograms were

(9) (a) Mdleleni, M. M.; Bridgewater, J. S.; Watts, R. J.; Ford, P. C. *Inorg. Chem.* **1995**, *34*, 2334. (b) Schmid, B.; Garces, F. O.; Watts, R. J. *Inorg. Chem.* **1994**, *33*, 9. (c) Craig, C. A.; Watts, R. J. *Inorg. Chem.* **1989**, *28*, 309. (d) Ichimura, K.; Kobayashi, T.; King, K. A.; Watts, R. J. *J. Phys. Chem.* **1987**, *91*, 6104. (e) Ohsawa, Y.; Sprouse, S.; King, K. A.; DeArmond, M. K.; Hanck, K. W.; Watts, R. J. *J. Phys. Chem.* **1987**, *91*, 1047.

(10) (a) Sprouse, S.; King, K. A.; Spellane, P. J.; Watts, R. J. *J. Am. Chem. Soc.* **1984**, *106*, 6647. (b) King, K. A.; Spellane, P. J.; Watts, R. J. *J. Am. Chem. Soc.* **1985**, *107*, 1431.

(11) Belser, P.; von Zelewsky, A. *Helv. Chim. Acta* **1980**, *63* (6), 1675.

(12) Constable, E. C.; Leese, T. A. *J. Organomet. Chem.* **1989**, *363*, 419.

obtained using a three-electrode cell system in a single compartment cell (30 mL capacity). All experiments employed a Pt disk working electrode in 0.1 M $(TBA)PF_6$ in CH_3CN referred to a Ag wire reference electrode (pseudoreference) with a Pt wire auxiliary electrode. The ferrocene/ferrocenium (Fc/Fc^+) couple was measured for each sample against the Ag wire pseudoreference; corrections were applied to all data according to $(E_{Pa} + E_{Pc})/2 = 400$ mV for the Fc/Fc^+ couple vs NHE.[13]

X-ray Structural Analyses. Layering pentane onto methylene chloride solutions of $[Au(dbbpy)(tdt)]PF_6$ and Au(η^2-*C,N*-ppy)(tdt) afforded yellow and orange needles, respectively, that were suitable for X-ray diffraction. Fragments of both $[Au(dbbpy)(tdt)]PF_6$ and Au(η^2-*C,N*-ppy)(tdt) were cut and mounted on glass fibers under Paratone-8277 and placed on the X-ray diffractometer in a cold nitrogen stream supplied by a Siemens LT-2A low-temperature device. The X-ray intensity data were collected on a standard Siemens SMART CCD area detector system equipped with a normal focus molybdenum-target X-ray tube operated at 2.0 kW (50 kV, 40 mA). A total of 1.3 hemispheres of data were collected using a narrow frame method with scan widths of 0.3° in ω and exposure times of 30 and 10 s/frame for $[Au(dbbpy)(tdt)]PF_6$ and Au(η^2-*C,N*-ppy)(tdt), respectively. Frames were integrated to 0.90 Å for $[Au(dbbpy)(tdt)]PF_6$ and to 0.75 Å for Au(η^2-*C,N*-ppy)(tdt) with the Siemens SAINT program yielding a total of 5538 reflections for $[Au(dbbpy)(tdt)]PF_6$ and 9282 reflections for Au(η^2-*C,N*-ppy)(tdt). The unit cell parameters were based upon the least-squares refinement of three-dimensional centroids of 2963 reflections and 5119 reflections at −80 and −90 °C for $[Au(dbbpy)(tdt)]PF_6$ and Au(η^2-*C,N*-ppy)(tdt), respectively. The space groups were assigned on the basis of systematic absences and intensity statistics by using the XPREP program (Siemens, SHELXTL 5.04). The structures were solved by direct methods (SHELXTL program, version 5.04) and refined by full-matrix least-squares on F^2. All non-hydrogen atoms for both structures were refined with anisotropic displacement parameters (except C(7) and C(7A) in $[Au(dbbpy)(tdt)]PF_6$) giving a data-to-parameter ratio of approximately 10:1. Anisotropic refinement of C(7) and C(7A) in Au(η^2-*C,N*-ppy)(tdt) resulted in unreasonably high thermal parameters, therefore these atoms were left isotropic. The disordered methyl group in the tdt ligand was modeled as an orientational disorder that refined to a site-occupancy factor of 60:40 and 50:50 for C(7):C(7A) in $[Au(dbbpy)(tdt)]PF_6$ and Au(η^2-*C,N*-ppy)(tdt), respectively. H atoms were included in the idealized positions for both structures. Crystallographic data for both structures are given in Table 1. Selected bond distances and angles are provided in Tables 2 and 3, and ORTEP representations of the structures are shown in Figures 1 and 3.

Results and Discussion

Syntheses. Diimine complexes of gold(III) have been known for some time[14] with the $[Au(diimine)Cl_2]^+$ cation being a useful starting material for subsequent preparations. However, the original syntheses of the chloride or perchlorate salts of $[Au(diimine)Cl_2]^+$, where diimine = 2,2′-bipyridine or 1,10-phenanthroline, gave rather poor yields (33 and <30%, respectively). While the poor solubility of the chloride salt made its use unfavorable, the explosive nature of perchlorate salts made the use of $[Au(diimine)Cl_2]ClO_4$ undesirable. In a more recent report,[12] the preparation of the $[AuCl_4]^-$ salt of the $[Au(diimine)Cl_2]^+$ cation was reported. An inherent difficulty with using this species for preparation of the corresponding diimine dithiolate complexes is the inevitable reaction of the $[AuCl_4]^-$ anion with the dithiolate salt. Metathesis reactions to substitute $[AuCl_4]^-$ with a nonreactive anion, e.g., PF_6^-, BF_4^-, and BPh_4^-, were unsuccessful. Thus, a new procedure for the preparation of $[Au(diimine)Cl_2]PF_6$ was developed. In a typical reaction, a solution of $K[AuCl_4]$ in water, which was saturated with KPF_6 (ca. 20 equiv), reacted with 1 equiv of the diimine in acetone solution to afford the diimine complex in high isolated yield as a pale yellow solid. For example, $[Au(dbbpy)Cl_2]PF_6$ (**1**) was prepared analytically pure in 88% yield. The ^1H NMR spectrum for **1** in DMSO-d_6 was consistent with the bidentate coordination of the dbbpy ligand, and integration of the resonances in the spectrum gave a 3:1 ratio of methyl-to-aromatic protons. The mass spectrum of the isolated powder exhibited a parent ion peak at *m*/*z* 535, consistent with the mass of the cation in **1**, and the isotopic pattern observed was nearly identical to the

Table 1. Crystal and Structure Refinement Data for $[Au(dbbpy)(tdt)]PF_6$ (**2**) and Au(η^2-*C,N*-ppy)(tdt) (**5**)

cryst params	**2**	**5**
chem formula	$C_{25}H_{30}AuF_6N_2PS_2$	$C_{18}H_{14}AuNS_2$
fw	764.57	505.39
space group (No.)	$P\bar{1}$ (2)	$P2_1/c$ (14)
Z	2	4
a, Å[a]	7.1977(2)	8.852(1)
b, Å	11.7292(1)	11.726(2)
c, Å	17.5820(5)	15.499(5)
α, deg	104.537(2)	
β, deg	96.592(2)	101.34(2)
γ, deg	102.455(2)	
V, Å^3	1380.41(6)	1577.5(6)
ρ_{calc}, g/cm^3	1.839	2.128
temp, °C	−80	−90
radiation, λ, Å	Mo, 0.710 73	Mo, 0.710 73
μ, mm^{-1}	5.597	9.585
$R_1(F_o)$, w$R_2(F_o^2)$, % ($I > 2\sigma(I)$)[b]	5.00, 10.62	4.38, 7.59
$R_1(F_o)$, w$R_2(F_o^2)$, % (all data)	6.94, 11.79	7.60, 13.17

[a] It has been noted that the integration program SAINT produces cell constant errors that are unreasonably small, since systematic error is not included. More reasonable errors might be estimated at 10× the listed values. [b] $R_1 = (\sum||F_o| - |F_c||)/\sum|F_o|$, w$R_2 = [\sum[w(F_o^2 - F_c^2)^2]/\sum[w(F_o^2)^2]]^{1/2}$, where $w = 1/[\sigma^2(F_o^2) + (aP)^2 + bP]$ and $P = [f(\text{max of } 0 \text{ or } F_o^2) + (1 - f)F_c^2]$.

Table 2. Selected Interatomic Distances (Å) and Bond Angles (deg) for $[Au(dbppy)(tdt)]PF_6$ (**2**)[a]

atoms	dist	atoms	angle
Au−N(1)	2.084(10)	N(1)−Au−S(1)	95.9(3)
Au−N(2)	2.068(9)	N(1)−Au−N(2)	79.4(4)
Au−S(1)	2.269(3)	N(2)−Au−S(2)	95.5(3)
Au−S(2)	2.264(3)	S(1)−Au−S(2)	89.20(12)
S(1)−C(1)	1.738(12)	N(1)−Au−S(2)	174.9(3)
S(2)−C(6)	1.776(13)	S(1)−Au−N(2)	175.1(3)
C(1)−C(6)	1.41(2)	Au−N(2)−C(13)	115.0(7)
N(1)−C(12)	1.38(2)	Au−N(1)−C(12)	114.7(7)
N(2)−C(13)	1.356(13)	Au−S(1)−C(1)	105.4(5)
C(12)−C(13)	1.48(2)	Au−S(2)−C(6)	104.8(4)

[a] Estimated standard deviations in the least significant figure are given in parentheses.

Table 3. Selected Interatomic Distances (Å) and Bond Angles (deg) for Au(η^2-*C,N*-ppy)(tdt) (**5**)[a]

atoms	dist	atoms	angle
Au−C(18)	2.035(7)	N(1)−Au−S(1)	95.8(2)
Au−N(1)	2.079(5)	N(1)−Au−C(18)	81.0(3)
Au−S(1)	2.342(2)	S(1)−Au−S(2)	89.72(8)
Au−S(2)	2.258(2)	S(2)−Au−C(18)	93.4(2)
S(1)−C(1)	1.759(7)	S(1)−Au−C(18)	176.9(2)
S(2)−C(6)	1.769(9)	N(1)−Au−S(2)	174.2(2)
C(1)−C(6)	1.392(12)	Au−C(18)−C(13)	112.7(5)
N(1)−C(12)	1.356(8)	Au−N(1)−C(12)	114.5(5)
C(12)−C(13)	1.464(10)	Au−S(1)−C(1)	102.8(3)
C(13)−C(18)	1.413(10)	Au−S(2)−C(6)	103.7(3)

[a] Estimated standard deviations in the least significant figure are given in parentheses.

(13) (a) Gritzner, G.; Kuta, J. *Pure Appl. Chem.* **1984**, *56* (4), 461. (b) Gagné, R. R.; Koval, C. A.; Lisensky, G. C. *Inorg. Chem.* **1980**, *19*, 2855.
(14) Harris, C. M.; Lockyer, T. N. *J. Chem. Soc.* **1959**, 3083.

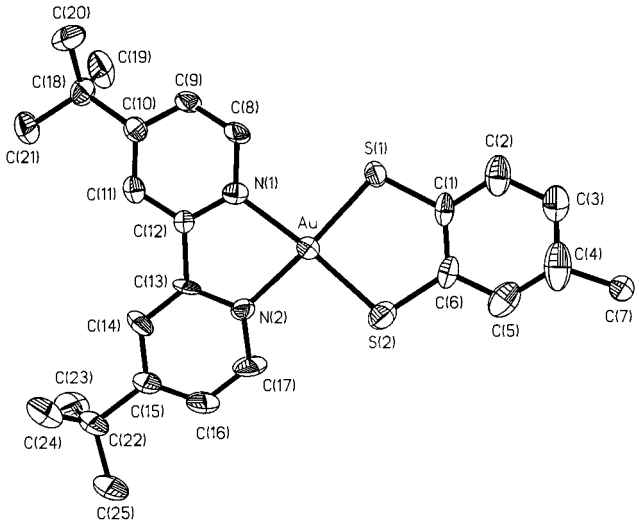

Figure 1. Molecular structure and atom-numbering scheme of the non-hydrogen atoms (ORTEP diagram, 50% thermal ellipsoids) of the cation in $[Au(dbbpy)(tdt)]PF_6$ (**2**).

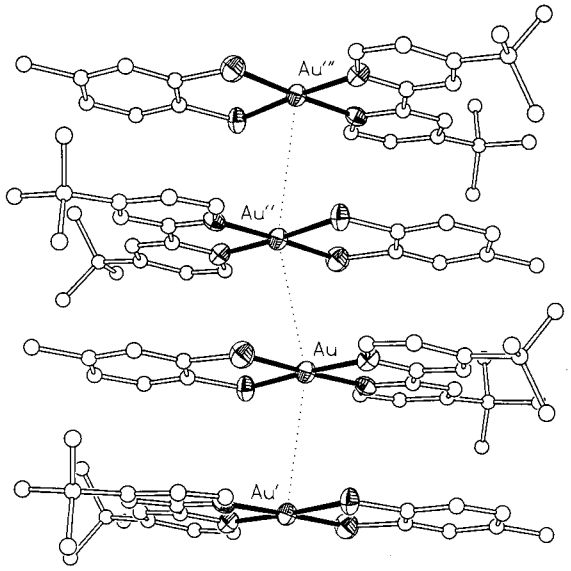

Figure 2. One repeat unit of the stacked array of the cation in **2** viewed perpendicular to the molecular planes and stacking axis. H atoms are not shown.

theoretical pattern calculated for this complex. This species is air-stable as a solid or in solution for extended periods of time.

Reaction of K_2tdt, which was prepared from KOH/MeOH and H_2tdt, with **1** at room temperature gave the complex $[Au(dbppy)(tdt)]PF_6$ (**2**) according to eq 1. Upon addition of the K_2tdt solution to a solution of **1** in CH_3CN, a brown precipitate, with a dark yellow supernatant, formed. The reaction mixture was stirred at room temperature for 2−3 h at which point the solvent was removed in vacuo and the residual solid extracted with CH_3CN and filtered. Subsequent crystallization from a CH_3CN/Et_2O mixture afforded complex **2** as deep-yellow needles in ca. 40% isolated yield.

The ^{1}H NMR spectrum of **2** shows the presence of a single methyl resonance and a single *t*-Bu resonance in a 1:6 ratio at δ 2.27 and 1.47, respectively. Although complex **2** lacks a C_2 axis, only a single set of resonances is observed for the dbbpy ligand with aromatic resonances shifted slightly upfield relative to the $[Au(dbbpy)Cl_2]PF_6$ precursor complex. There is a single set of aromatic resonances consistent with the tdt ligand. The

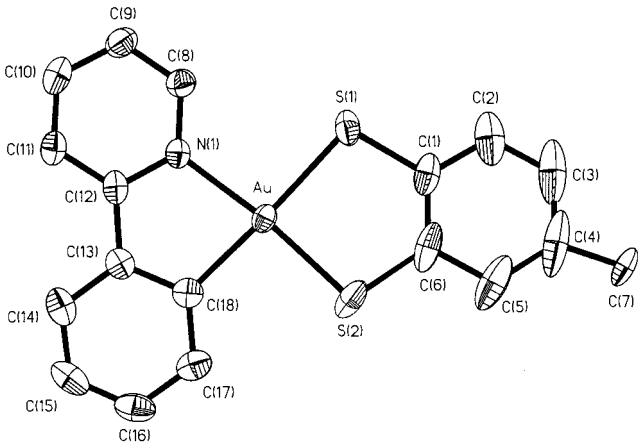

Figure 3. Molecular structure and atom-numbering scheme of the non-hydrogen atoms (ORTEP diagram, 50% thermal ellipsoids) of Au(η^2-*C*,*N*-ppy)(tdt) (**5**).

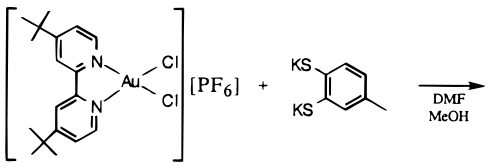

1

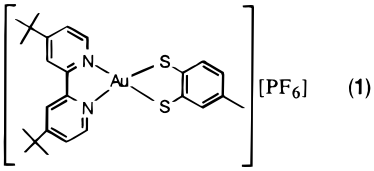

2 (1)

solid-state IR spectrum in a KBr pellet shows a prominent absorption band at 830 cm^{-1} and a weaker absorption band at 550 cm^{-1}, both characteristic of PF_6^-.[15] Recrystallization of the solid from CH_2Cl_2/hexanes gave an analytically pure product, the FDMS of which shows a strong parent ion peak at *m*/*z* 619, consistent with the cation $[Au(dbppy)(tdt)]^+$, and a second, less intense peak at *m*/*z* 764, which is consistent with the mass of the ion pair, $\{[Au(dbppy)(tdt)]PF_6\}$. The polyisotopic patterns for both the cation and the ion pair match their calculated mass spectra. The solid-state structure for **2** was determined and is discussed below. Complex **2** is air stable as a solid for extended periods of time and is moderately stable in solution. A DMSO-d_6 solution was exposed to air for several days without any change in its ^{1}H NMR spectrum.

The preparation of the orthometalated complex, Au(η^2-*C*,*N*-ppy)Cl_2 (**3**), by the transmetalation reaction of $\{(\eta^2$-*C*,*N*-ppy)-$HgCl\}_n$ with $K[AuCl_4]$ has been described previously by Constable and Leese.[12] They have also described an alternative preparation of **3** by thermolysis of a CH_3CN/H_2O solution of Au(η^1-*N*-ppy)Cl_3 (**4**) at reflux temperature. This latter reaction did not proceed as described, however, and **4** was recovered quantitatively when the thermolysis reaction was attempted. On the other hand, a TGA scan of **4** in flowing N_2 showed a clean thermal decomposition to the expected orthometalated species, **3**, with a weight loss corresponding to 1 equiv of HCl. The onset of degradation was at 150 °C and continued until 220

(15) (a) Nakamoto, K. *Infrared and Raman Spectra of Inorganic and Coordination Compounds*, 4th ed.; Wiley: New York, 1986. (b) Serra, O. A.; Perrier, M.; Lakatos Osorio, V. K.; Kawano, Y. *Inorg. Chim. Acta* **1976**, *17*, 135. (c) Beck, W. *Inorg. Synth.* **1990**, *28*, 1.

°C; so it appears that a higher temperature than that of CH_3CN/H_2O at reflux is required to activate the ortho C−H bond and form the orthometalated complex, **3**. The resultant species was stable to 360 °C at which point onset of decomposition to elemental gold occurred. Complex **3** is stable indefinitely in air as a solid and is stable in solution for at least several days.

The complex Au(η^2-*C*,*N*-ppy)(tdt) (**5**) was synthesized in a reaction of **3** with K_2tdt in MeOH at room temperature according to eq 2 to give a mixture of two isomers. The isomers are

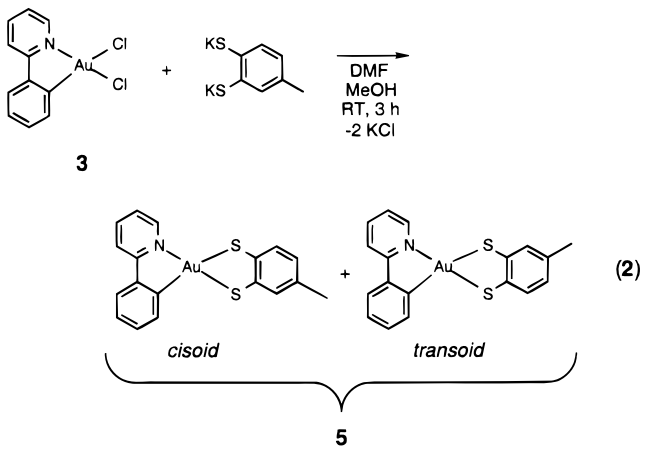

distinguished by the position of the coordinated phenyl-*C* atom relative to the tdt methyl substituent (*cisoid* or *transoid*). The product was obtained in 68% yield following crystallization from DMF/Et_2O at −18 °C. The ^{1}H NMR spectrum of complex **5** shows several aromatic proton resonances consistent with the nonsymmetric ppy ligand as well as two sets of aromatic proton resonances for the tdt ligand. Two overlapping methyl resonances at δ 2.24 and 2.23 in an apparent ratio of ca. 1:1 correspond to the presence of the two isomers shown in eq 2. The recrystallized product is analytically pure. A field desorption mass spectrum shows a parent ion peak at *m*/*z* 505 consistent with the mass of complex **5** and its calculated mass spectrum. The solid-state structure for **5** has been determined and is discussed below. The complex is air stable as a solid indefinitely and air stable in solution for several days. A DMSO-d_6 solution was left exposed to air for 4 days without any change in its ^{1}H NMR spectrum.

Solid-State Structures. In complex **2** (Figure 1), the Au(III) ion exhibits the expected square planar coordination geometry characteristic of d^8 metal complexes. The metal ion and the ligand donor atoms are essentially coplanar with negligible deviation from the plane. The two Au−N diimine bonds are the same, within experimental error, averaging 2.076 Å, which is shorter than the corresponding distance in [Au(bpy)$(mes)_2$]$^+$ (2.125(6) Å)[7] but longer than that found in [Au(bpy)Cl_2]$^+$ (2.037(13) Å).[16] The observed differences arise from differences in the trans influence of the S, C, and Cl donors in the three complexes. The Au−S bonds are also the same, within experimental error, averaging 2.27 Å, and significantly shorter than those in the bis(dithiolate) complex, Bu_4N[Au(tdt)$_2$] (2.30−2.32 Å).[17] The Au−S distances in **2** are, however, similar to the Pt−S distances in the analogous Pt(II) complexes, Pt(bpy)(bdt)[18a] (2.247 Å), where bdt = benzenedithiolate, and Pt(Me_2bpy)(met)[18b] (2.245 Å), where Me_2bpy = 4,4′-dimethyl-2,2′-bipyridine and met = dimethylmaleate-1,2-dithiolate.

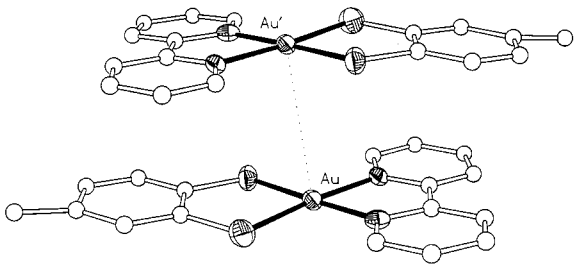

Figure 4. One repeat unit of the stacked array of **5** viewed perpendicular to the molecular planes and stacking axis. H atoms are not shown.

The square planar coordination geometry in **2** deviates slightly from perfect 90° bond angles owing to constraints of the chelating diimine ligand with a N(1)−Au−N(2) angle of 79.4(4)° and a consequent N(1)−Au−S(1) angle of 95.9(3)°. The S(1)−Au−S(2) angle is nearly ideal at 89.20(12)°. The overall planarity of the molecule favors stacking in the solid state, and this can be seen in Figure 2. The molecules stack in an alternating arrangement such that the diimine ligand moiety in one molecule lies above the dithiolate ligand moiety in the other, and *vice versa*. The Au···Au vectors form a slightly zigzag arrangement with intermolecular Au···Au distances of 3.60 and 3.75 Å alternating between neighboring molecules. The Au···Au distances are as long or longer than that found in the [Au(η^3-*C*,*N*,*N*-dpp)Cl]$^+$ cations (3.6 Å),[8] but are much shorter than the nearest intermolecular Au···Au distance in systems such as [Au(bpy)Cl_2]BF_4 (6.85 Å).[16] The distance of 3.6 Å is, however, too long to indicate significant intermolecular bonding between neighboring complexes.[19]

Complex **5** (Figure 3) exhibits square planar coordination geometry similar to that observed for complex **2**. Again, the metal and four ligand atoms, CNSS in this case, are essentially coplanar with negligible deviation from the plane. Complex **5** differs from **2** in that it has a Au−C σ-bond. The Au−N distance (2.079(5) Å) is nearly identical to those in **2**, and the Au−C distance (2.035(7) Å) is similar to other Au−C distances, e.g., in Au(damp-*C*,*N*)(mnt) (2.038(6) Å),[20] where damp-*C*,*N* = 2-(*N*,*N*-dimethylaminomethyl)phenyl and mnt = maleonitriledithiolate, and Au(η^2-*C*,*N*-phenyloxazoline)Cl_2 (2.040(8) Å).[21] The most notable structural feature in complex **5** is the difference in Au−S bond lengths. The Au−S(1) distance (2.342(2) Å), which is trans to the Au−C bond, is longer than the Au−S(2) distance (2.258(2) Å) trans to the pyridyl N by ca. 0.1 Å as a result of a structural trans effect. The bond lengths in Au(damp-*C*,*N*)(mnt) are comparable, with a Au−S distance of 2.363(2) Å trans to the Au−C bond and a Au−S distance of 2.270(2) Å trans to the Au−N bond.[20] As in complex **2**, the square planar geometry in complex **5** deviates from ideality due to chelate ring constraints with a N(1)−Au−C(18) angle of 81.0(3)° and a N(1)−Au−S(1) angle of 95.8°. The S(1)−Au−S(2) angle is nearly ideal at 89.72(8)°.

The overall planarity of **5** results in stacking of molecules in the solid state (Figure 4), with Au···Au vectors showing a slightly zigzag arrangement. The molecules stack in a manner such that the phenylpyridine ligand in one molecule lies above

(16) McInnes, E. J. L.; Welch, A. J.; Yellowless, L. J. *Acta Crystallogr., Sect. C* **1995**, *C51*, 2023.
(17) Mazid, M. A.; Razi, M. T.; Sadler, P. J. *Inorg. Chem.* **1981**, *20*, 2872.
(18) (a) Connick, W. B.; Gray, H. B. *J. Am. Chem. Soc.* **1997**, *119*, 11620. (b) Bevilacqua, J. M.; Eisenberg, R. *Inorg. Chem.* **1994**, *33*, 2913.
(19) Mingos, D. M. P. *J. Chem. Soc., Dalton Trans.* **1996**, 561.
(20) Mack, J.; Ortner, K.; Abram, U.; Parish, R. V. *Z. Anorg. Allg. Chem.* **1997**, *623*, 873.
(21) Bonnardel, P. A.; Parish, R. V.; Pritchard, R. G. *J. Chem. Soc., Dalton Trans.* **1996**, 3185.

Table 4. Room-Temperature Electronic Spectral Data for Gold(III) Complexes[a]

complex	nm	$10^{-3}\nu$, cm^{-1}	ϵ_{max} (M^{-1} cm^{-1})
[Au(dbbpy)(tdt)]PF_6 (**2**)	444	22.5	2310
	320 (sh)	31.3	9670
	294 (sh)	34.0	10970
	230	43.4	13980
Au(η^2-*C*,*N*-ppy)(tdt) (**5**)	406	24.5	3170
	328 (sh)	30.5	4025
	310 (sh)	32.3	5230
	224	44.6	6550
[Au(dbbpy)Cl_2]PF_6 (**1**)	302	33.1	8240
	276 (sh)	36.2	7800
	228	43.9	10200
Au(η^2-*C*,*N*-ppy)Cl_2 (**3**)	334	29.9	3140
	292	34.2	3940
	224	44.6	4800
dbbpy	292	34.3	3970
	232	43.1	5230
2-ppy	290	34.5	1050
	234	42.7	1410

[a] All spectra were recorded in CH_2Cl_2.

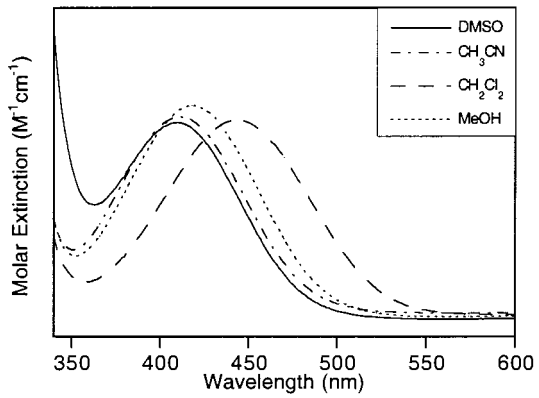

Figure 5. Solvatochromic absorption band in [Au(dppby)(tdt)]PF_6 (**2**).

the dithiolate ligand of its nearest neighbor. The Au···Au′ distance of 3.81 Å is slightly longer than those in **2**.

Electronic Absorption and Emission Spectroscopy. The electronic absorption spectroscopic data for **1**−**3** and **5** are presented in Table 4. The absorption spectrum of **2** in CH_2Cl_2 consists of very intense absorption bands in the near-ultraviolet (UV) spectral region with maxima at 230, 294, and 320 nm (ϵ = 13 980, 10 970, and 9670 M^{-1} cm^{-1}, respectively) and a weaker, low-energy band at 444 nm (ϵ, 2310 M^{-1} cm^{-1}). This low-energy band is slightly sensitive to solvent and shifts to λ_{max} at 410 nm (ϵ, 2285 M^{-1} cm^{-1}) in DMSO (Figure 5). Except for the low-energy band at 444 nm, these absorptions are nearly identical in shape and close in extinction coefficient to those of the precursor complex [Au(dbbpy)Cl_2]PF_6 (**1**), although the energies are very slightly shifted to higher values. An absorption spectrum of the free ligand, dbbpy, in CH_2Cl_2 reveals similar high-energy bands with maxima at 232 (ϵ, 5230 M^{-1} cm^{-1}) and 292 (ϵ, 3970 M^{-1} cm^{-1}) nm. The high-energy absorptions, therefore, can be attributed to the diimine ligand and can be assigned as $\pi-\pi^*$ transitions which are perturbed by complexation to the Au(III) center. In comparison, Zn(II) α,α'-diimine complexes,[22] which are known to exhibit only intraligand $\pi-\pi^*$ transitions, have high-energy absorption bands consistent with those in **1** and **2**. The high-energy absorption bands in Pt(II) diimine complexes[23] and in Pt(bpy)(bdt),[18a] where bdt = benzenedithiolate, have also been attributed to intraligand $\pi-\pi^*$ transitions of the diimine ligand and provide additional support for the assignment of the high-energy bands in **1** and **2**. The slightly higher intensities of the high energy bands possibly suggest that transitions involving the tdt ligand in **2** may overlap in this region. The low-energy charge-transfer band at 444 nm (CH_2Cl_2) is mildly solvatochromic but occurs at higher energy and with weaker intensity than is found in the neutral Pt(II) analogue, Pt(dbbpy)(tdt) (λ_{max} (CH_2Cl_2) = 563 nm; ϵ, 7200 M^{-1} cm^{-1}).[6a] The possible effect of metal complex charge on this transition can be gauged by comparing the analogous CT transition for the cationic complex [Pt(Me_2bpy)(Et_2dtc)]$^+$,[18b] where Me_2bpy = 4,4′-dimethyl-2,2′-bipyridine and Et_2dtc = diethyldithiocarbamate, with that for the neutral species Pt(Me_2bpy)(ecda),[6c] where ecda = 1-(ethoxycarbonyl)-1-cyanoethylene-2,2-dithiolate. The former exhibits a band at 380 nm in $CHCl_3$ that shows modest solvent dependence, whereas the latter has a more solvatochromic charge transfer that occurs at 492 nm in CH_2Cl_2. The similarity of the low-energy CT transition in **2** to that seen for the corresponding Pt(II) systems leads to a tentative assignment of the lowest-energy excited state in this complex as a charge-transfer-to-diimine transition.

Complex **2** is not emissive in either fluid solution or in a low-temperature glass matrix with $\lambda_{excit} \geq 300$ nm. On the other hand, its precursor complex, **1**, emits strongly at 77 K in a DMM glass matrix although it is not emissive in fluid solution. The 77 K emission is vibronically structured with maxima at 427, 455, 479, and 515 (sh) nm. The vibrational spacings are consistent with ring breathing modes in the aromatic diimine ligand and originate from a lowest intraligand ($\pi-\pi^*$) excited state. The relative energies of the emission are consistent with those of Yam et al.,[7] who assigned the structured emission observed from [Au(dpphen)Cl_2]$^+$ as an intraligand diimine $\pi-\pi^*$ transition.

Analogous to the absorption spectra for **2** and its related precursor, **1**, the near-UV spectrum for **5** also possesses strong absorption maxima in the UV region at 224, 310, and 328 nm (ϵ = 6550, 5230, and 4025 M^{-1} cm^{-1}, respectively) in CH_2Cl_2. There is also a low-energy band centered at 406 nm (ϵ, 3170 M^{-1} cm^{-1}) which is tentatively assigned as a charge-transfer-to-diimine transition. It is mildly sensitive to solvent with λ_{max} ranging from 394 nm (ϵ, 3185 M^{-1} cm^{-1}) in DMSO to 428 nm (ϵ, 3365 M^{-1} cm^{-1}) in toluene. This solvatochromic transition is higher in energy and less intense than that of the Pt(II) analogues. Regarding the higher energy absorptions for **5**, the dichloride complex **3** also exhibits moderately intense bands at 224, 292, and 334 nm (ϵ = 4800, 3940, and 3140 M^{-1} cm^{-1}, respectively), as does the free ligand, ppy, with bands at 234 and 290 nm (ϵ = 1410 and 1050 M^{-1} cm^{-1}, respectively). The high-energy bands for **5** can thus be attributed to ligand centered $\pi-\pi^*$ transitions, as well. By analogy, the high-energy absorption transitions (240−340 nm) in Pd(ppy)L_2 complexes are also assigned as intraligand $\pi-\pi^*$ transitions localized on the 2-phenylpyridinate ligand.[9c] Similar to **2**, the relatively higher intensities of the high-energy bands possibly suggest that transitions involving the tdt ligand in **5** may overlap in this region, as well.

As in complex **2**, no emission is observed for complex **5** in fluid solution or in a low-temperature glass matrix. Similarly, no emission is observed for the dichloride precursor, **3**, in fluid

(22) (a) Bray, R. G.; Ferguson, J.; Hawkins, C. J. *Aust. J. Chem.* **1969**, *22*, 2091. (b) Ohno, T.; Kato, S. *Bull. Chem. Soc. Jpn.* **1974**, *47*, 2953. (c) Flynn, C. M.; Demas, J. N. *J. Am. Chem. Soc.* **1974**, *96*, 1959.

(23) Miskowski, V. M.; Houlding, V. H. *Inorg. Chem.* **1989**, *28*, 1529.

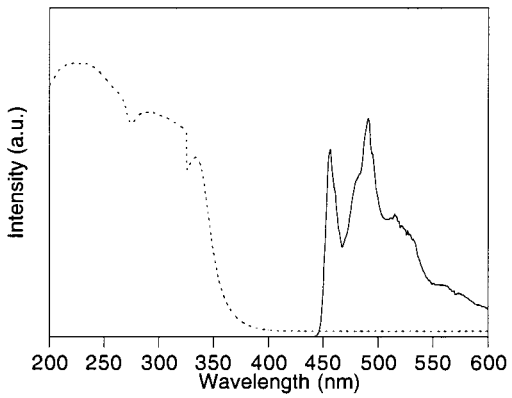

Figure 6. Absorption (···) at 298 K and emission (—) at 77 K spectra of Au(η-*C,N*-ppy)Cl_2 (**5**) in a DMM glass matrix.

Table 5. Summary of Cyclic Voltammetry for Complexes [Au(dbbpy)(tdt)]PF_6 (**2**) and Au(η^2-*C,N*-ppy)(tdt) (**5**)[a]

complex	$\mathbf{E}'_{p,red}$ (V)	ΔE_p (V)	$E'_{p,ox}$ (V)	ΔE_p (V)	i_{pc}/i_{pa}
[Au(dbbpy)(tdt)]PF_6 (**2**)	−0.255		1.589		
	−1.539	0.124			
Au(η^2-*C,N*-ppy)(tdt) (**1**)	−1.339		0.925	0.132	0.8

[a] A correction was applied to all reported potential values to bring measured potentials in acetonitrile vs the Ag-wire pseudoreference electrode to potentials vs NHE (corrected according to $(E_{pc} + E_{pa})/2$ for $Fc/Fc^+ = 400$ mV).

solution, but an intense emission is observed in a low-temperature glass matrix (Figure 6). The emission is highly structured (λ_{max} 456, 490, 517, 527, and 559 nm) with C═C and C═N vibrational modes of the ppy ligand. In a recent study by Ford and co-workers,[9a] similar spectra were observed for Pt(II) complexes with orthometalated 2-phenylpyridinate as a ligand (λ_{max} 476, 512, and 542 nm). In the absorption spectrum for Pt(η^2-*C,N*-ppy)(CO)Cl, for example, there is a solvent sensitive MLCT band at ca. 380 nm and they attributed the observed emission to a MLCT state. There is no corresponding absorption feature in the spectrum of **3**; therefore, any analogous MLCT transition in the Au(III) system must lie at least 3000 cm^{-1} to higher energy, buried beneath the ligand centered CT bands. The origin of the emission for Pt(η^2-*C,N*-ppy)(CO)Cl in a 77 K glassy solution is ca. 1000 cm^{-1} lower in energy than that for the emission in **3**. Since the emission in **3** is not as strongly shifted as the MLCT absorption band, if it does indeed exist, our results are more consistent with a $\pi-\pi^*$ assignment for the emissive state of **3**. It should be noted that the Huang−Rhys ratio *S* for **3** is ∼1.2 as compared to ∼0.8 for Ford's Pt(II) complex, Pt(η^2-*C,N*-ppy)(CO)Cl, also consistent with enhanced $\pi-\pi^*$ character in **3** relative to the Pt(II) systems.[23]

Electrochemistry. Cyclic voltammograms of both Au(III) tdt complexes, **2** and **5**, were obtained in CH_3CN with (TBA)-PF_6 as the supporting electrolyte, and the electrochemical data are summarized in Table 5. An irreversible reduction wave was observed at −0.255 V for the cationic complex **2** while a similar irreversible reduction wave was seen for the ppy complex **5** at a significantly more negative potential, −1.339 V. The diimine complex **2** also exhibits an irreversible oxidation at 1.589 V, while the phenylpyridine complex **5** undergoes a quasi-reversible oxidation at a significantly less positive potential with $E_{p,ox} = 0.925$ V ($\Delta E_p = 0.124$ V). These observations are consistent with the expectation that a cationic complex is easier to reduce and harder to oxidize than a neutral analogue. On the basis of the assignment given above for the low-energy charge-transfer band, it appears that the positive charge on **2** serves to stabilize the π^* diimine LUMO significantly relative to that for **5** and related neutral Pt(dbbpy)(dithiolate) complexes[6a] so that reduction occurs at much less negative potential for **2**. The more facile oxidation of **5** relative to **2** results from the greater σ-donation of the ppy ligand that serves to raise the energy of the HOMO, as well as from the difference in charge between the two complexes.

Nature of the Lowest Excited States in the Au(III) Complexes 2 and 5. While most of the data presented above can be accommodated on the basis of the electronic structural model used to analyze the neutral Pt(II) diimine dithiolate complexes reported previously,[6] the absence of luminescence and the effect of changing from Pt(II) to Au(III) make further analysis of the excited-state structures of **2** and **5** necessary. The fact that the Pt(II) diimine tdt complexes show solution luminescence consistent with a mixed metal/dithiolate-to-diimine charge transfer raises a question of why this emission is not seen for **2** and **5** if the same electronic structural model is adopted. It is also relevant that the cationic complex [Au(dbbpy)Cl_2]$^+$ exhibits a high-energy $\pi-\pi^*$ emission at 77 K but neither tdt complex, **2** or **5**, does. The change from Pt(II) to Au(III) in square-planar diimine dithiolate complexes clearly has a major impact on d-orbital energies and spatial extent (and hence overlap) that will affect the frontier orbitals and associated states in ways not fully comprehended at this point. If the same electronic structural model exists in **2** and **5** as is found in the Pt(II) diimine dithiolate analogues, then some mechanism has led to a substantial increase in the rate of nonradiative decay (k_{nr}) so that luminescence is not observed. On the other hand, the change in d-orbital energies and overlap integrals may lead to a change in the lowest lying excited state. For example, if the σ^* orbital, d_{xy}, becomes close in energy or even drops below the π^* diimine level in going from Pt(II) to Au(III) and the other d orbitals become correspondingly more stable leading to greater dithiolate character in the HOMO, then low-lying, nonemissive ligand-to-metal charge-transfer becomes a distinct possibility. Further investigation into the electronic structure of Au(III) diimine dithiolates appears warranted.

Summary

The complexes [Au(dbbpy)(tdt)]PF_6 (**2**) and Au(η^2-*C,N*-ppy)-(tdt) (**5**) were synthesized to investigate their emission properties and the effect of the metal, Au vs Pt, on luminescence behavior. The structures of both complexes were established by single-crystal X-ray structure determinations, and their spectroscopic properties were examined. The complexes, **2** and **5**, both exhibit square planar coordination geometries. Absorption spectra for **2** and **5** reveal a mildly solvatochromic, low-energy charge transition which is higher in energy and significantly lower in intensity than the Pt(II) congeners and is attributed to a charge-transfer-to-diimine excited state. However, no emission is observed from this excited state in fluid solution or in rigid media at low temperature. The dichloride precursor complexes, **1** and **3**, are emissive at low temperature in a glass matrix, and the emissive state is tentatively assigned as an intraligand $\pi-\pi^*$ in both. The dramatic difference in the spectroscopy observed with Au(III) relative to its Pt(II) analogues emphasizes the role of the metal in the lowest energy excited states of the Pt(II) complexes.

Acknowledgment. We wish to thank the National Science Foundation through its grant to the Science and Technology Center for Photoinduced Charge Transfer (CHE-9120001) for support of this research. Dr. W. B. Connick is thanked for helpful discussions.

Supporting Information Available: X-ray crystallographic files, in CIF format, for complexes **2** and **5** are available on the Internet only. Access information is given on any current masthead page.

IC980032B